Published OnlineFirst June 30, 2009; DOI: 10.1158/0008-5472.CAN-09-0718

Priority Report

# Protein Kinase D Regulates Cell Migration by Direct Phosphorylation of the Cofilin Phosphatase Slingshot 1 Like

**Philipp Peterburs, Johanna Heering, Gisela Link, Klaus Pfizenmaier, Monilola A. Olayioye, and Angelika Hausser**

Institute of Cell Biology and Immunology, University of Stuttgart, Stuttgart, Germany

## Abstract

**Protein kinase D (PKD) has been identified as a negative regulator of epithelial cell migration; however, its molecular substrates and downstream signaling pathways that mediate this activity have remained elusive. In this study, we provide evidence that the cofilin phosphatase slingshot 1 like (SSH1L), an important regulator of the complex actin remodeling machinery, is a novel *in vivo* PKD substrate. PKD-mediated phosphorylation of serines 937 and 978 regulates SSH1L subcellular localization by binding of 14-3-3 proteins and thus impacts the control of local cofilin activation and actin remodeling during cell migration. In line with this, we show that the loss of PKD decreases cofilin phosphorylation, induces a more spread cell morphology, and stimulates chemotactic migration of breast cancer cells in an SSHL1-dependent fashion. Our data thus identify PKD as a central regulator of the cofilin signaling network via direct phosphorylation and regulation of SSH1L.** [Cancer Res 2009;69(14):5634–8]

## Introduction

The protein kinase D (PKD) family of serine/threonine kinases consists of three isoforms: PKD1, PKD2, and PKD3 (1). Our recent work shows that active PKD localizes to the leading edge and directly interacts with filamentous-actin (F-actin) *in vitro* (2), making it very likely that PKD is involved in the regulation of actin remodeling, a fundamental aspect of cell migration and invasion. Indeed, wild-type (WT) PKD strongly inhibited migration of pancreas and prostate cancer cells, whereas dominant-negative PKD significantly increased cell migration (2, 3). In this study, we show that PKD directly phosphorylates and regulates slingshot (SSH) 1 like (SSH1L), a phosphatase that activates the actin depolymerizing protein cofilin by dephosphorylation. Cofilin nucleates actin polymerization by severing actin filaments to generate free barbed ends and also increases the rate of actin depolymerization, thus maintaining a pool of actin monomers (4, 5). Cofilin phosphorylation by LIM kinases and testicular protein kinase at serine 3 turns off the actin-binding activity of cofilin and thus leads to inactivation. Accordingly, dephosphorylation by the SSH as well as chronophin phosphatases results in reactivation of the actin binding activity of cofilin (6). The cofilin phosphatase SSH1L is an ubiquitously expressed phosphatase implicated in diverse cellular processes such as regulation of membrane protrusions and mitosis (7). The interaction of SSH1L with F-actin is a prerequisite for its activation and required for the chemotactic response of cells (8). 14-3-3 proteins associate with SSH1L when phosphorylated at serines 937 and 978, thereby sequestering SSH1L in the cytoplasm and preventing translocation of the phosphatase to F-actin–rich membrane protrusions (9). The kinase responsible for phosphorylation of serines 937 and 978, however, has not been identified. We now provide evidence that PKD1 and PKD2 directly phosphorylate SSH1L at these residues, thereby controlling SSH1L localization and thus cofilin dephosphorylation and activation at membrane protrusions. Accordingly, PKD controls migration of breast cancer cells via the SSH1L-cofilin signaling pathway.

## Materials and Methods

**DNA constructs, reagents, and antibodies.** Full-length human SSH1L cDNA was amplified by PCR using the RZPD clone IRAUp969F0865D6 as a template and cloned into pCR3.V62-Met-Flag and pEGFP-N3 vectors. The SSH1L point mutant was generated by site-directed PCR mutagenesis. Integrity of all constructs was verified by sequencing. Antibodies used were as follows: anti-PKD2 rabbit polyclonal antibody (Calbiochem), anti-PKD C-20 (Santa Cruz Biotechnology), anti–phospho-cofilin (Ser3) and anti-cofilin rabbit polyclonal antibodies (Cell Signaling), anti-Flag M2 mouse monoclonal antibody (Sigma-Aldrich, Germany), anti-tubulin mouse monoclonal antibody (Neomarkers), anti-SSH1L rabbit polyconal antibody (Abcam), and anti–glutathione *S*-transferase (GST) goat polyclonal antibody (GE Healthcare). Secondary antibodies used were horseradish peroxidase–coupled donkey anti-goat, goat anti-mouse, and anti-rabbit IgGs (Dianova). Alexa546- and Alexa633-coupled phalloidin were from Invitrogen.

**Cell culture.** Cells were maintained in RPMI 1640 supplemented with 10% FCS. COS7 and HEK293T cells were transfected with Lipofectamine 2000 (Invitrogen) and TransIT293 (Mirus), respectively. In the case of siRNA oligonucleotides, cells were transfected with Oligofectamine (Invitrogen). siRNA oligonucleotides used were 5′-gucgagagaagaggucaaatt-3′ (PKD1), 5′-gcaaagacugcaaguuuaatt-3′ (PKD2 #1), 5′-ggacaucaaugaccagauctt-3′ (PKD2 #2), and 5′-ucgucacccaagaaagauatt-3′ (SSH1L). As a control, a lacZ-specific siRNA was used (5′-gcggcugccggaauuuacctt-3′). Protein extraction of cells, GST pulldowns, and Western blotting were performed as described (10).

**Immunofluorescence microscopy.** Staining of cells was performed as described (11). Cells were imaged with a 40.0×/1.25 HCX PL APO objective lens on a confocal laser scanning microscope (TCS SP2; Leica). The average area covered by a single cell was calculated using Axiovision software (Zeiss). Identical microscopic settings (image size, 1,024 × 1,024 pixel and 375 × 375 μm) were applied. At least 70 cells were analyzed per sample. Images shown are stacks of several confocal sections.

**Kinase assay.** Flag-SSH1L was immunoprecipitated from cell lysates of HEK293T cells transiently expressing Flag-SSH1L with Flag-M2-Agarose (Sigma-Aldrich), eluted from the beads with 100 nmol/L glycine (pH 2.5), and neutralized using 1.5 mol/L Tris (pH 8.8). PKD1 WT, PKD1kd, PKD2-Flag WT, and PKD2kd-Flag were precipitated from lysates of transfected HEK293T cells using PKD-specific antibodies. Kinase assays using purified Flag-SSH1L as a substrate were carried out as described (10).

**Transwell assays.** Cell migration assays were performed as described (11) with the following modifications: MCF7 and MDA-MB-231 cells were

**Requests for reprints:** Angelika Hausser, University of Stuttgart, Allmandring 31, 70569 Stuttgart, Germany. Phone: 497116856-6995; Fax: 497116856-7484; E-mail: angelika.hausser@izi.uni-stuttgart.de.

©2009 American Association for Cancer Research.

doi:10.1158/0008-5472.CAN-09-0718



Downloaded from cancerres.aacrjournals.org on November 17, 2019. © 2009 American Association for Cancer Research.

Published OnlineFirst June 30, 2009; DOI: 10.1158/0008-5472.CAN-09-0718



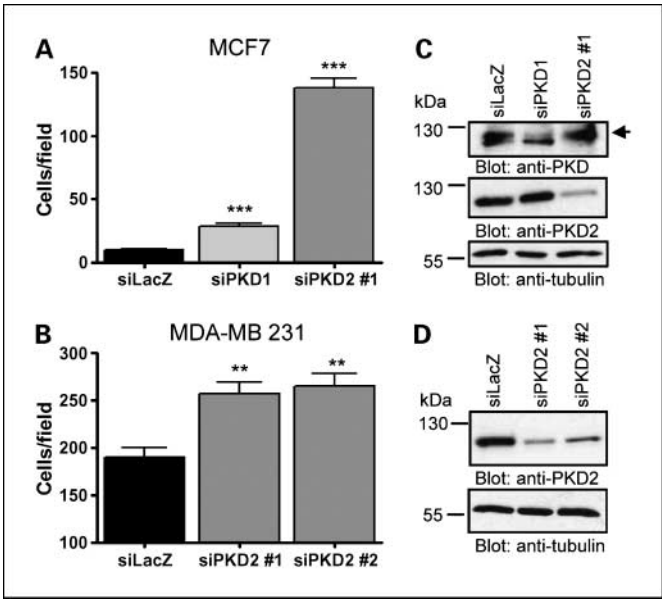


**Figure 1.** Depletion of PKD1 and PKD2 enhances migration of MCF7 and MDA-MB 231 cells. MCF7 (*A*) and MDA-MB 231 cells (*B*) transfected with siRNAs specific for PKD1, PKD2, or with LacZ-specific control siRNA were allowed to migrate across a Transwell filter. *Columns,* mean of duplicate wells and representative of three independent experiments; *bars,* SE. **, $P < 0.01$; ***, $P < 0.0001$. *C* and *D,* silencing efficiency in siRNA-transfected cells was verified by immunoblotting. *Arrow,* PKD1. Equal loading was verified by detection of tubulin.

seeded at a density of 100.000 cells per insert and 25.000 cells per insert, respectively. Migration was induced by a FCS gradient of 0% to 10% for 4 h (MDA-MB-231) or 0.5% to 10% for 16 h (MCF7). The significance of differences was analyzed by unpaired Student's *t* test.

## Results and Discussion

To address whether PKD regulates directed migration of breast cancer cells, we used the poorly invasive MCF7 and highly invasive MDA-MB 231 cell lines. Reverse transcription-PCR (RT-PCR) analysis and Western blotting revealed that MCF7 cells express both PKD1 and PKD2, whereas MDA-MB 231 cells express only PKD2 (data not shown). We depleted PKD1 and PKD2 in these cells using specific siRNAs and measured cell motility in Transwell assays. In MCF7 cells, the loss of PKD1 stimulated migration 3-fold compared with the siLacZ control, whereas the loss of PKD2 enhanced migration up to 10-fold (Fig. 1*A*). Specific down-regulation of the PKD proteins was verified by immunoblotting (Fig. 1*C*). Due to the lack of a PKD1-specific antibody, we used an antibody that crossreacts with both PKD1 and 2. The antibody detected a double band, with the slower migrating band representing PKD1 and the faster one representing PKD2 (Fig. 1*C, top*). Thus, in lysates from cells transfected with PKD1- and PKD2-specific siRNA, the respective protein band is absent, proving their specific and successful depletion. Consistent with the results in MCF7 cells, down-regulation of PKD2 using two specific siRNAs significantly enhanced cell migration of MDA-MB 231 cells (Fig. 1*B*). Specific down-regulation of the PKD2 protein was again verified by immunoblotting (Fig. 1*D*). Of note, compared with MCF7 cells, depletion of PKD2 in MDA-MB 231 cells was not as effective in terms of stimulating cell migration, which is likely due to their high basal migratory properties (Fig. 1*A* and *B*). The fact that depletion of PKD2 in MCF7 cells enhanced cell migration more efficiently than the loss of PKD1 could suggest that the kinases signal via different target proteins. Alternatively, it is possible that PKD2 is the predominantly expressed isoform. Indeed, RT-PCR and Western blot analysis of different breast carcinoma cell lines revealed ubiquitous expression of PKD2, whereas PKD1 was differentially expressed (data not shown).

In migrating cells, actin polymerization drives the formation and extension of the lamellipodial leading edge. PKD1 and PKD2 directly interact with F-actin at these sites, suggesting that PKD negatively regulates migration of cells by modulating proteins of the actin cytoskeleton machinery (2). We thus examined morphology and F-actin distribution of MCF7 cells lacking either PKD1

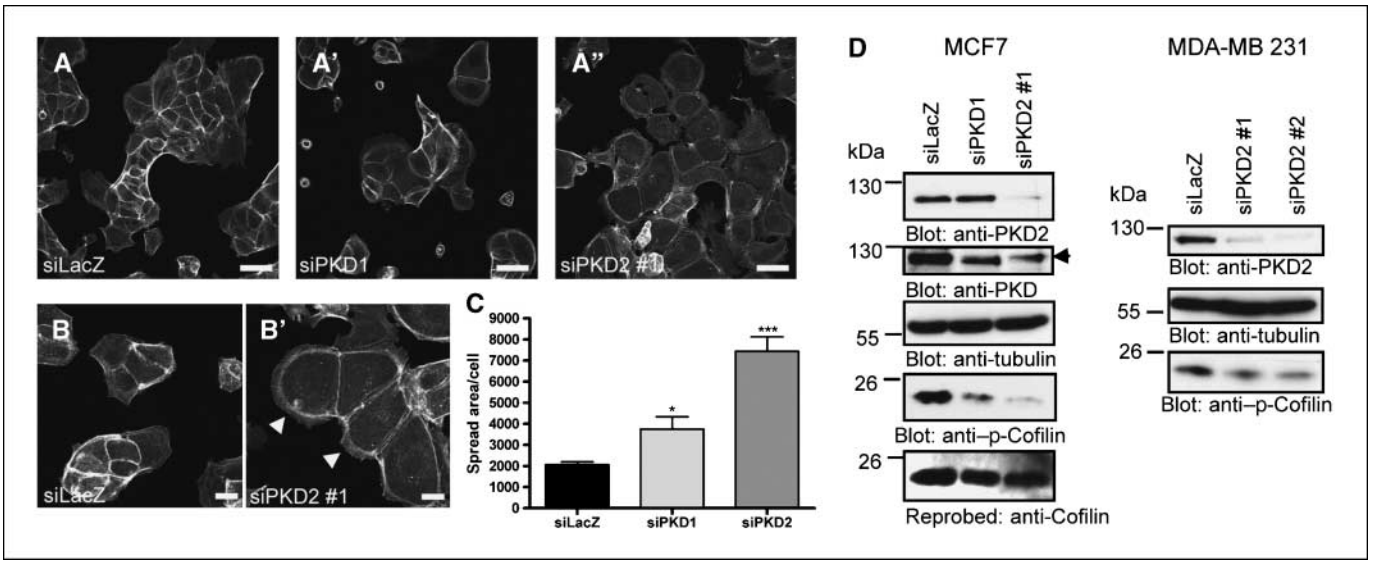


**Figure 2.** Depletion of PKD modulates cell morphology and decreases cofilin phosphorylation. *A* and *B,* MCF7 cells transfected with the indicated siRNA were replated onto collagen-coated coverslips and stained with Alexa546-coupled phalloidin. *Arrows,* F-actin–positive membrane protrusions. *Scale bar,* 50 μm (*A, A'*, and *A''*) and 20 μm (*B* and *B'*). *C,* the average area covered by a single cell was calculated as described in the methods section. *Columns,* mean area/cell in $\mu m^2$; *bars,* SE. Four independent microscopic fields were analyzed. *, $P < 0.05$; ***, $P < 0.0001$. *D,* cofilin phosphorylation and PKD depletion was analyzed by immunoblotting. Equal loading was verified by detection of tubulin and cofilin (MCF7). *Arrow,* PKD1.



Downloaded from cancerres.aacrjournals.org on November 17, 2019. © 2009 American Association for Cancer Research.

Published OnlineFirst June 30, 2009; DOI: 10.1158/0008-5472.CAN-09-0718



or PKD2. Control cells displayed a typical rounded morphology (Fig. 2*A*). Depletion of PKD1 had only minor effects on cell morphology, with cells appearing slightly more spread out (Fig. 2*A'*). Depletion of PKD2, however, caused the cells to appear with a circular and drastically spread morphology (Fig. 2*A"*). Calculation of the average area covered by a single cell (Fig. 2*C*) showed that depletion of PKD1 and PKD2 led to a 2- and 4-fold increase of the cell area, respectively. Furthermore, cells lacking PKD2 displayed more prominent F-actin–positive lamellipodial structures when compared with control cells (Fig. 2*B, B', arrows*). One of the key proteins in the formation of membrane protrusions and directional migration is cofilin, which is known to promote actin remodeling. Interestingly, epidermal growth factor–induced cofilin activation is accompanied by an increase in cell area resulting from protrusion (12). We thus investigated whether PKD is involved in the regulation of cofilin phosphorylation and activation. Indeed, depletion of either PKD1 or PKD2 in MCF7 and MDA-MB-231 cells resulted in decreased cofilin phosphorylation when compared with control cells (Fig. 2*D*). Depletion of PKD2 was again more effective than depletion of PKD1, which is consistent with the enhanced migratory potential of cells lacking PKD2.

Cofilin dephosphorylation at serine 3 is executed by chronophin (13) and the members of the SSH family, SSH1L, SSH2L, and SSH3L (14, 15). SSH1L is recruited to and activated at F-actin–rich structures at the leading edge of migrating cells. SSH1L activity is inhibited by interaction with 14-3-3 proteins, which is dependent on the phosphorylation of serines 937 and 978 (9). These two serines match the PKD consensus motif (Fig. 3*A*), which is characterized by a leucine, isoleucine, or valine residue in the -5 and arginine in the -3 position relative to a serine or threonine. We therefore performed *in vitro* kinase assays using PKD1 WT, PKD2 WT, and kinase dead (kd) PKD proteins together with purified Flag-SSH1L as a substrate. SSH1L was efficiently phosphorylated by PKD1 WT and PKD2 WT but not the kd proteins (Fig. 3*B*), proving that PKD can use SSH1L as a substrate. Inhibition of PKD-mediated phosphorylation should result in enhanced interaction of SSH1L with F-actin and reduced binding to 14-3-3 proteins. Localization of GFP-SSH1L WT was predominantly cytoplasmic, whereas the S937/978A mutant was mainly associated with F-actin in COS7 cells (Fig. 3*C*). Coexpression of dominant-negative PKD2kd, indeed, directed SSH1L WT to F-actin structures (Fig. 3*C*). Furthermore, depletion of PKD2 from MDA-MB 231

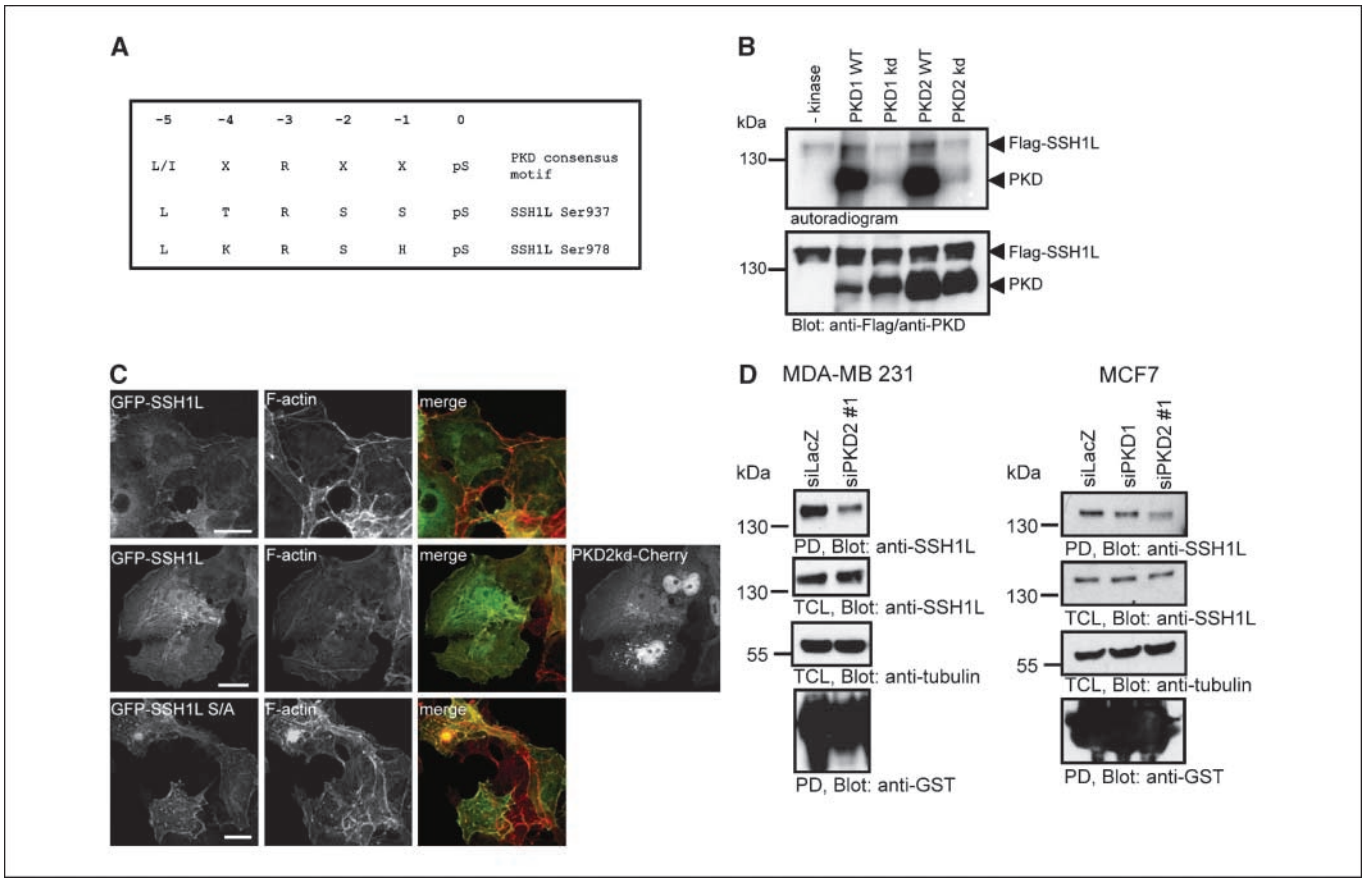


**Figure 3.** PKD-mediated phosphorylation of SSH1L regulates localization and interaction with 14-3-3 proteins. *A,* alignment of the PKD consensus motif and the two potential PKD motifs in SSH1L. *B,* purified Flag-SSH1L was incubated in kinase buffer containing [$^{32}$P]-γ-ATP in the absence (- *kinase*) and presence of PKD1 WT, PKD1kd, PKD2 WT, and PKD2kd. Incorporation of radioactive phosphate was analyzed using a PhosphoImager (*top*), followed by immunoblotting with Flag- and PKD-specific antibodies (*bottom*). *C,* COS-7 cells transfected with GFP-SSH1L WT, GFP-SSH1L-S937/978A (S/A), and GFP-SSH1L WT plus PKD2kd-Cherry were stained with Alexa633-phalloidin. *Scale bar,* 20 μm. *D,* cells were transfected with siRNAs as indicated, lysed, and incubated with GST-14-3-3β coupled to glutathione sepharose beads. Bound proteins were detected with an SSH1L-specific antibody. Expression of SSH1L and equal protein loading was verified by immunoblotting with SSH1L- and tubulin-specific antibodies, respectively. Detection of GST-fusion proteins using a GST-specific antibody served as a control. *PD,* pulldown.



Downloaded from cancerres.aacrjournals.org on November 17, 2019. © 2009 American Association for Cancer Research.

Published OnlineFirst June 30, 2009; DOI: 10.1158/0008-5472.CAN-09-0718



and MCF7 cells clearly reduced the interaction of SSH1L with 14-3-3β, and depletion of PKD1 also had a minor effect in MCF7 cells (Fig. 3*D*). These results confirm that PKD regulates interaction of SSH1L with 14-3-3 proteins and SSH1L localization by direct phosphorylation, thereby controlling the local dephosphorylation and activation of cofilin. In mammary breast cancer cells, initial cofilin activation was shown to require the release of the protein from the PM by a PLCγ-mediated decrease in PtIns(4, 5)$P_2$ levels (12, 16). Consequently, depending on cell type and stimulus, dephosphorylated cofilin is not necessarily active. We therefore analyzed whether depletion of SSH1L could restore cofilin phosphorylation and suppress cell migration of cells lacking PKD2. Indeed, in MDA-MB 231 (Fig. 4*C*) and MCF7 (Fig. 4*D*) cells, cofilin phosphorylation was restored when both proteins were down-regulated. Accordingly, migration of these cells was comparable with control cells (Fig. 4*A* and *B*). These findings confirm that stimulation of migration in PKD-depleted cells is due to enhanced activity of SSH1L. siRNA-mediated knockdown of SSH1L has been reported to inhibit directional migration of chemokine-stimulated T cells and platelet-derived growth factor (PDGF)–induced smooth muscle cells (8, 17). In line with this, we observed reduced migration and enhanced cofilin phosphorylation upon SSH1L depletion in MDA-MB 231 cells (Fig. 4*C*). However, migration of MCF7 cells was not affected by SSH1L down-regulation (Fig. 4*B*), indicating that the low basal migratory potential of these cells does not require SSH1L.

Stimulation of cells with growth factors such as heregulin activates SSH1L by dephosphorylation and induces its translocation to the F-actin compartment (9). Likewise, PKD is activated by PDGF or serum stimulation and recruited to the leading edge where it directly interacts with F-actin (2). PKD-mediated phosphorylation and inactivation of SSH1L is thus likely to occur at the F-actin compartment where both proteins localize. In contrast, dephosphorylation and activation of SSH1L takes place in the cytoplasm (9). However, phosphorylation and dephosphorylation of SSH1L have to be tightly coordinated not only in a spatial but also in a temporal manner to ensure a polarized pattern of cofilin activation. Based on our results, we propose that PKD controls directional cell migration by phosphorylation of SSH1L. This in turn induces binding of SSH1L to 14-3-3 proteins, thereby abrogating its interaction with F-actin and resulting in cytosolic sequestration of SSH1L. This shifts the balance toward an inactive phosphorylated pool of cofilin, which does not favor cell migration. The identification of PKD as a crucial component of this cofilin signaling network is an important step toward the understanding of the molecular mechanisms controlling coordinated directional cell migration.

**Addendum.** While this article was under review, Eiseler and colleagues (18) described an essential role for PKD1 in cofilin-mediated F-actin regulation via SSH1. Because the authors used HeLa cells in which PKD1 and PKD2 were depleted as a cellular model, the question whether the two PKD isoforms act redundantly or whether one isoform is dominant over the other with respect to cofilin regulation remains unresolved.

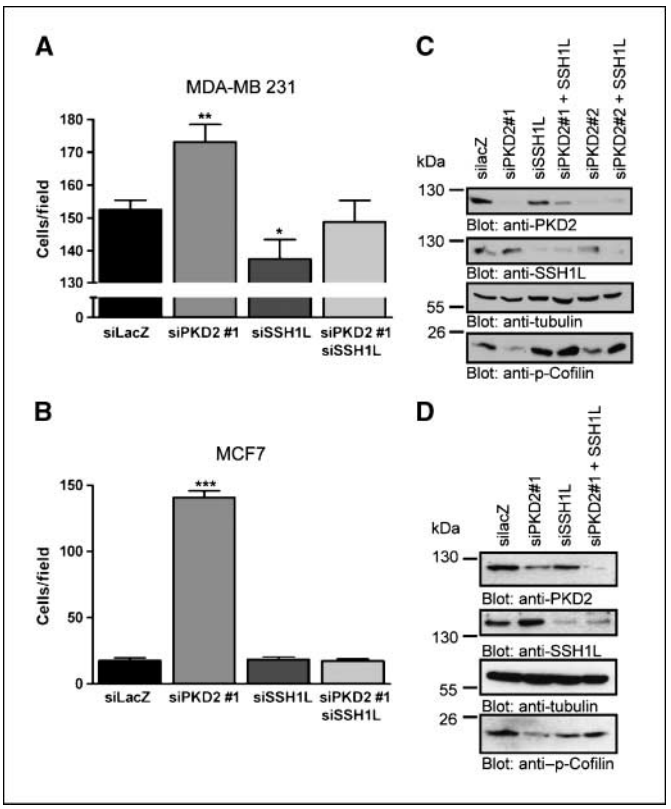


**Figure 4.** SSH1L depletion restores cofilin phosphorylation and reduces migration of cells lacking PKD2. Migration of MDA-MB 231 (*A*) and MCF7 cells (*B*) transfected with the indicated siRNAs. *Columns,* mean of duplicate wells and representative of at least two independent experiments; *bars,* SE. *, $P < 0.05$; **, $P < 0.01$; ***, $P < 0.0001$. *C* and *D,* cofilin phosphorylation and expression of SSH1L and PKD2 in siRNA-transfected cells was analyzed by immunoblotting. Equal loading was verified by detection of tubulin. A representative blot is shown ($n = 3$).

## Disclosure of Potential Conflicts of Interest

No potential conflicts of interest were disclosed.

## Acknowledgments

Received 2/25/09; revised 4/28/09; accepted 6/3/09; published OnlineFirst 6/30/09.

**Grant support:** Center Systems Biology Stuttgart (project A1) and the Heidelberger Akademie der Wissenschaften (WIN-Kolleg).

The costs of publication of this article were defrayed in part by the payment of page charges. This article must therefore be hereby marked *advertisement* in accordance with 18 U.S.C. Section 1734 solely to indicate this fact.

## References

1. Wang QJ. PKD at the crossroads of DAG and PKC signaling. Trends Pharmacol Sci 2006;27:317–23.
2. Eiseler T, Schmid MA, Topbas F, Pfizenmaier K, Hausser A. PKD is recruited to sites of actin remodelling at the leading edge and negatively regulates cell migration. FEBS Lett 2007;581:4279–87.
3. Jaggi M, Rao PS, Smith DJ, et al. E-cadherin phosphorylation by protein kinase D1/protein kinase C{mu} is associated with altered cellular aggregation and motility in prostate cancer. Cancer Res 2005;65:483–92.
4. Andrianantoandro E, Pollard TD. Mechanism of actin filament turnover by severing and nucleation at different concentrations of ADF/cofilin. Mol Cell 2006;24:13–23.
5. Ichetovkin I, Grant W, Condeelis J. Cofilin produces newly polymerized actin filaments that are preferred for dendritic nucleation by the Arp2/3 complex. Curr Biol 2002;12:79–84.
6. Wang W, Eddy R, Condeelis J. The cofilin pathway in breast cancer invasion and metastasis. Nat Rev Cancer 2007;7:429–40.
7. Plastino J, Sykes C. The actin slingshot. Curr Opin Cell Biol 2005;17:62–6.
8. Nishita M, Tomizawa C, Yamamoto M, Horita Y,



Downloaded from cancerres.aacrjournals.org on November 17, 2019. © 2009 American Association for Cancer Research.

Published OnlineFirst June 30, 2009; DOI: 10.1158/0008-5472.CAN-09-0718



Ohashi K, Mizuno K. Spatial and temporal regulation of cofilin activity by LIM kinase and Slingshot is critical for directional cell migration. J Cell Biol 2005; 171:349–59.

**9.** Nagata-Ohashi K, Ohta Y, Goto K, et al. A pathway of neuregulin-induced activation of cofilin-phosphatase Slingshot and cofilin in lamellipodia. J Cell Biol 2004; 165:465–71.

**10.** Scholz RP, Regner J, Theil A, et al. DLC1 interacts with 14-3-3 proteins to inhibit RhoGAP activity and block nucleocytoplasmic shuttling. J Cell Sci 2009;122:92–102.

**11.** Holeiter G, Heering J, Erlmann P, Schmid S, Jahne R, Olayioye MA. Deleted in liver cancer 1 controls cell migration through a Dia1-dependent signaling pathway. Cancer Res 2008;68:8743–51.

**12.** van Rheenen J, Song X, van Roosmalen W, et al. EGF-induced PIP2 hydrolysis releases and activates cofilin locally in carcinoma cells. J Cell Biol 2007;179: 1247–59.

**13.** Gohla A, Birkenfeld J, Bokoch GM. Chronophin, a novel HAD-type serine protein phosphatase, regulates cofilin-dependent actin dynamics. Nat Cell Biol 2005;7: 21–9.

**14.** Niwa R, Nagata-Ohashi K, Takeichi M, Mizuno K, Uemura T. Control of actin reorganization by Slingshot, a family of phosphatases that dephosphorylate ADF/ cofilin. Cell 2002;108:233–46.

**15.** Ohta Y, Kousaka K, Nagata-Ohashi K, et al. Differential activities, subcellular distribution and tissue expression patterns of three members of Slingshot family phosphatases that dephosphorylate cofilin. Genes Cells 2003;8:811–24.

**16.** van Rheenen J, Condeelis J, Glogauer M. A common cofilin activity cycle in invasive tumor cells and inflammatory cells. J Cell Sci 2009;122:305–11.

**17.** San Martin A, Lee MY, Williams HC, Mizuno K, Lassegue B, Griendling KK. Dual regulation of cofilin activity by LIM kinase and Slingshot-1L phosphatase controls platelet-derived growth factor-induced migration of human aortic smooth muscle cells. Circ Res 2008; 102:432–8.

**18.** Eiseler T, Doppler H, Yan IK, Kitatani K, Mizuno K, Storz P. Protein kinase D1 regulates cofilin-mediated F-actin reorganization and cell motility through slingshot. Nat Cell Biol 2009;11:545–56.



Downloaded from cancerres.aacrjournals.org on November 17, 2019. © 2009 American Association for Cancer Research.

Published OnlineFirst June 30, 2009; DOI: 10.1158/0008-5472.CAN-09-0718

Cancer Research
The Journal of Cancer Research (1916–1930) | The American Journal of Cancer (1931–1940)

AACR American Association for Cancer Research

# Protein Kinase D Regulates Cell Migration by Direct Phosphorylation of the Cofilin Phosphatase Slingshot 1 Like

Philipp Peterburs, Johanna Heering, Gisela Link, et al.

*Cancer Res* 2009;69:5634-5638. Published OnlineFirst June 30, 2009.

**Updated version** Access the most recent version of this article at: doi:10.1158/0008-5472.CAN-09-0718

**Cited articles** This article cites 18 articles, 8 of which you can access for free at: http://cancerres.aacrjournals.org/content/69/14/5634.full#ref-list-1

**Citing articles** This article has been cited by 29 HighWire-hosted articles. Access the articles at: http://cancerres.aacrjournals.org/content/69/14/5634.full#related-urls

**E-mail alerts** Sign up to receive free email-alerts related to this article or journal.

**Reprints and Subscriptions** To order reprints of this article or to subscribe to the journal, contact the AACR Publications Department at pubs@aacr.org.

**Permissions** To request permission to re-use all or part of this article, use this link http://cancerres.aacrjournals.org/content/69/14/5634. Click on "Request Permissions" which will take you to the Copyright Clearance Center's (CCC) Rightslink site.

Downloaded from cancerres.aacrjournals.org on November 17, 2019. © 2009 American Association for Cancer Research.